

NACA TN 3018

NATIONAL ADVISORY COMMITTEE FOR AERONAUTICS

TECHNICAL NOTE 3018

A THEORETICAL STUDY OF THE EFFECT OF FORWARD SPEED ON THE
FREE-SPACE SOUND-PRESSURE FIELD AROUND PROPELLERS

By I. E. Garrick and C. E. Watkins

Langley Aeronautical Laboratory
Langley Field, Va.

LIBRARY COPY

JUL 1 1988

LANGLEY RESEARCH CENTER
LIBRARY NASA
HAMPTON, VIRGINIA

FOR REFERENCE

NOT TO BE TAKEN FROM THIS ROOM



Washington

October 1953



NATIONAL ADVISORY COMMITTEE FOR AERONAUTICS

TECHNICAL NOTE 3018

A THEORETICAL STUDY OF THE EFFECT OF FORWARD SPEED ON THE
FREE-SPACE SOUND-PRESSURE FIELD AROUND PROPELLERS

By I. E. Garrick and C. E. Watkins

SUMMARY

The sound-pressure field of a rotating propeller in forward flight in free space is analyzed by replacing the normal-pressure distribution over the propeller associated with thrust and torque by a distribution of acoustic pressure doublets acting at the propeller disk and subject to uniform rectilinear motion. The basic element used to synthesize the field is the pressure field of a concentrated force moving uniformly at subsonic speeds, for which an expression generalizing one of Horace Lamb's for the fixed concentrated force is given. This result is presented both for the moving and for the fixed observer. The strength of the doublet distribution is related to the thrust and torque distribution in a convenient but approximate way. The sound field is expressed by integration over the propeller disk, and also by integration over an effective ring, and is given both for the near pressure field and, in a simpler form, for the far field. Known results for the zero-forward-speed case present themselves in the special case of Mach number $M = 0$. Some illustrative examples are calculated and discussed.

INTRODUCTION

The rotating propeller is the source of an intense sound-pressure field which can be associated with the periodic reactions on the medium arising from the distribution of pressure rotating along with the blades. This pressure distribution consists in part of a distribution due to thickness of the blades, whose resultant force in subsonic potential flow is zero, and in part a distribution due to angle of attack and camber of the blades whose integrated effect includes the induced drag and corresponds almost wholly to the thrust and torque distribution over the blade. Another source of propeller noise may be associated with flow separation and with friction or shear due to the boundary layer; both effects lead to vorticity shed into the wake and hence the designation vortex noise. The vortex noise and the noise due to thickness (where wave drag is not a large factor) are, however, for actual propellers normally of a considerably smaller magnitude than the rotational sound due to torque and

thrust; hence only the latter effect will be considered in the present work.

A large number of investigators have studied various phases of the determination of the sound or noise field of rotating propellers. In addition to the references cited, a bibliography is included of representative work on this subject. A simplification that has frequently been made in propeller-noise investigations is to limit the considerations to the static or standing propeller. The work of Gutin in 1936 (ref. 1) represents a development of this type that makes possible a satisfactory prediction of the amplitude of sound pressure due to thrust and torque of a propeller rotating on a stand in still air. Although Gutin's theory is applicable to the near oscillating-pressure field of the propeller, his results in reference 1 are limited to the determination of the fundamental and the first few harmonics at a distance far from the propeller, that is, several diameters away. The determination of the near pressure field, however, has been of concern both from structural and physiological considerations. Hubbard and Regier (ref. 2) extended the application of Gutin's work to describe the oscillating pressure field and to determine the amplitude of noise at points near the propeller, in some cases within a blade chord length from the tip. They investigated analytically the effect of several of the parameters that enter in the theory and also gave comparisons with experiment which were quite satisfactory.

The existing theoretical work has found useful application for static conditions and for conditions of low forward speed, for example, near take-off. For conditions of high forward speeds, however, many pertinent questions have arisen as to the possible effects of the forward speed on the oscillating pressure field of the propeller. A few investigators have examined phases of this problem; Bryan, Hart, Shirokov, Blokhintzev, and particularly Kuessner and Billings (see bibliography) may be mentioned, but most of this work seems incomplete or difficult to apply. It appeared desirable, especially for applications, to reexamine the theoretical problem for the propeller at forward speed so as to have it arise as a straightforward generalization of existing work for the zero-forward-speed case. The purpose of the present paper is therefore to extend the theory of Gutin (ref. 1) and the work of Hubbard and Regier (ref. 2) so as to include the effect of subsonic forward speed of the propeller on the near and the far oscillating sound-pressure field caused by torque and thrust of the propeller.

This paper includes the following material: (a) The sound-pressure field associated with a uniformly moving concentrated force is given with details of the explicit development contained in the appendix. This result serves as a basic element for synthesizing the total pressure field. It is expressed both for the case of the observer or field point considered to be moving along rectilinearly and uniformly with the propeller in free space and for the case of the observer considered fixed

and the propeller in uniform flight. (b) The disturbance forces associated with the pressure distribution acting on the medium in the plane of the propeller disk are presented in the manner similar to that of Gutin. (c) The sound-pressure field resulting from the combined use of (a) and (b) is shown in the form requiring integrations over the propeller disk and in the simpler form making use of an effective propeller radius. Approximations valid for the far field, which reduce to Gutin's results for the case of zero forward speed, are also given. (d) Some numerical examples are calculated and discussed. (e) Remarks on the usefulness and limitations of the analysis.

SYMBOLS

$A(r)$	chordwise distribution of thrust acting on a radial element of a propeller blade
B	number of propeller blades
$b(r)$	width of propeller blades
c	velocity of sound
C_P	power coefficient, $P/\rho n^3 D^5$
C_T	thrust coefficient, $T/\rho n^2 D^4$
D	propeller diameter
$F(r)$	chordwise distribution of forces perpendicular to the thrust of a propeller blade and giving rise to the torque
F_x, F_y, F_z	components of force vector \bar{F}
$k = \frac{\omega}{c}$	
J_{mB}	Bessel function of first kind with index mB
M	Mach number, V/c
m	order of harmonic
n	propeller rotational speed, rps

P	power
p	pressure
p	pressure magnitude
p_Q	pressure due to torque
p_T	pressure due to thrust
p_{rms}	root-mean-square pressure
Q	torque
R	length of propeller blades
R_e	effective length of propeller blades
r	radius to a blade element
r, θ	polar coordinates in yz-plane
$s = \sqrt{(x - x_1)^2 + \beta^2 [(y - y_1)^2 + (z - z_1)^2]}$	
$s_o = \sqrt{x^2 + \beta^2 y^2}$	
$s = \sqrt{(x - x_1)^2 + (y - y_1)^2 + (z - z_1)^2}$	
$s_o = \sqrt{x^2 + y^2}$	
s_o, ϕ	polar coordinates in xy-plane
T	thrust
t	time
V	forward velocity
x, y, z	Cartesian coordinates

$$\beta = \sqrt{1 - M^2}$$

β_R blade angle

η propeller efficiency

ρ fluid density

$$\sigma = \frac{M(x - x_1) + S}{\beta^2}$$

$$\tau = \frac{b}{r\Omega}$$

τ_0 period, $2\pi/B\Omega$

Ω angular velocity

ω frequency of mth harmonic, $mB\Omega$

ω_1 fundamental frequency, $B\Omega$

ANALYSIS

Extension of a Formula in Lamb's "Hydrodynamics" for the
Sound-Pressure Field of a Fixed Concentrated Force
to That of a Moving Force

On the basis of acoustic considerations of the classical hydrodynamic equations, Lamb (ref. 3) gives the pressure at any field point x, y, z associated with an external periodic force $Ae^{i\omega t}$ acting in the x -direction and concentrated at the location x_1, y_1, z_1 as

$$p = \frac{A}{4\pi} \frac{\partial}{\partial x} \frac{e^{i\omega(t - \frac{s}{c})}}{s} \quad (1)$$

where

$$s = \sqrt{(x - x_1)^2 + (y - y_1)^2 + (z - z_1)^2} \quad (2)$$

The concentrated force may be regarded as stemming from the limit of a distribution of an increasing pressure difference over a decreasing area, whose product in the limit of zero area is equal to the force. For an arbitrary concentrated force of components F_x , F_y , F_z the result generalizes as Lamb indicates to

$$p = \frac{1}{4\pi} \left[\frac{\partial}{\partial x} \frac{F_x(t - \frac{s}{c})}{s} + \frac{\partial}{\partial y} \frac{F_y(t - \frac{s}{c})}{s} + \frac{\partial}{\partial z} \frac{F_z(t - \frac{s}{c})}{s} \right] \quad (3)$$

This formula shows that the pressure field obtained from the concentrated force has the character of a doublet or a dipole¹; in its periodic form it has played a central role in the development of the noise and pressure fields of propellers due to the propeller torque and thrust. However, the formula refers to a concentrated force and to coordinates fixed in space. To treat the case involving effects of forward speed, it is expedient to obtain the required extension of the preceding formula.

The extension of equation (3) required for the case of a uniformly moving concentrated force is given in equation (4), which follows. Details for its derivation are supplied in the appendix. Let the concentrated force have components F_x , F_y , F_z ; let it be moving uniformly with velocity V in the direction of the positive x -axis; and let the coordinate system also move uniformly with the same velocity. Then, with x , y , z now denoting the field point referred to this coordinate system and with x_1 , y_1 , z_1 denoting the coordinates of the concentrated moving force

$$p = \frac{1}{4\pi} \left[\frac{\partial}{\partial x} \frac{F_x(t - \frac{\sigma}{c})}{s} + \frac{\partial}{\partial y} \frac{F_y(t - \frac{\sigma}{c})}{s} + \frac{\partial}{\partial z} \frac{F_z(t - \frac{\sigma}{c})}{s} \right] \quad (4)$$

where

$$\left. \begin{aligned} s &= \sqrt{(x - x_1)^2 + \beta^2 [(y - y_1)^2 + (z - z_1)^2]} \\ \sigma &= \frac{M(x - x_1) + s}{\beta^2} \\ \beta &= \sqrt{1 - M^2} \end{aligned} \right\} \quad (5)$$

¹Since the acoustical pressure is $p = -\rho \frac{\partial \phi}{\partial t}$, the dipole is an acceleration doublet or the time rate of change of a flow doublet.

Figure 1 illustrates the geometric meaning of the quantities s , S , and σ . The force located at $O(x_1, y_1, z_1)$ and the field point at $Q(x, y, z)$ are both in uniform motion with velocity V in the x -direction. The distance $\overline{OQ} = s$. The influence at Q at time t stems from the action of the force when it was at position P , where P is obtained from the relation $\overline{OP}/\overline{OQ} = M$, the forward-speed Mach number. The distance \overline{PQ} gives then directly the phase radius σ . The perpendicular dropped from O onto PQ determines \overline{QR} , which is equal to the amplitude radius S . For $M = 0$ both S and σ reduce to the ordinary radius s . Comparison of equations (3) and (4) shows that the effect of the forward speed leads to replacement of s by S in the amplitude and by σ in the phase.

The force variation of main concern herein is that of a harmonically periodic force \overline{F} having components F_x, F_y, F_z varying in time as $e^{i\omega t}$. Equation (4) becomes

$$p = \frac{1}{4\pi} \left(F_x \frac{\partial}{\partial x} + F_y \frac{\partial}{\partial y} + F_z \frac{\partial}{\partial z} \right) \frac{e^{-ik\sigma}}{S} \quad (6)$$

where $k = \omega/c$. Equation (6) is the basic relation to be made use of in the subsequent analysis.

Disturbance Forces in the Propeller Plane

Consider as does Gutin (ref. 1) a propeller disk oriented so that the axis passing through the center of the disk coincides with the x -axis and let the propeller be assumed to rotate, as in figure 2, in the yz -plane ($x = 0$) with positive values of x corresponding to points ahead of (and negative values of x corresponding to points behind) the propeller disk. The propeller is considered to move uniformly with velocity V in the positive x -direction. Points in the propeller disk are designated by $(0, y_1, z_1)$, or, in polar coordinates (as shown in fig. 2), by

$$\left. \begin{aligned} y_1 &= r \cos \theta \\ z_1 &= r \sin \theta \end{aligned} \right\} \quad (7)$$

For definiteness, let the propeller be rotating counterclockwise as seen by an observer looking into the propeller toward the slipstream.

Each element of the propeller is acted on by the surface pressure distribution and this distribution may be resolved into a thrust force in the direction of the axis of rotation (the x-axis) and into a force associated with the torque which acts about the axis of rotation opposing the rotation. Equal and opposite reaction forces to these are exerted on the medium. The points of application of these forces are imagined to act in a single plane designated as the plane of rotation or as the propeller disk.

The reaction of the surface pressure distribution of the rotating propeller on the medium at any instant is to be replaced by fixed periodic forces acting at the propeller disk. The propeller disk itself will be considered covered with the necessary singularities in the pressure or acoustic radiators of proper strength and harmonic content to correspond to this normal-pressure distribution. These singularities will be seen to be acceleration sources (acoustic radiator of zero order) for those forces which act symmetrically on both sides of the blade, that is, whose net force over each element of the blade is zero, and to be acceleration doublets (acoustic radiator of order one) for those forces acting antisymmetrically, that is, whose net force over each element of the blade corresponds to the difference in pressure over both sides of the blade. The doublet distribution is that which is needed to represent the thrust and torque distribution, in particular that part of the thrust and torque distribution associated with pressures acting normal to the blade surface. This part is practically all of it, except that arising from skin friction. (The effect of blade thickness may be taken into account by introducing either flow sources or acceleration sources: the flow sources would lead to the sound-pressure field due to thickness by the classical "piston" effect of the moving blade on the flow field; the acceleration sources would deal directly with the assumed or known contribution to the pressure distribution over the blade due to thickness.)

Consider an element of the propeller at distance r from the axis; let dr be its radial length and b its width measured in the projection onto the plane of rotation. Let the forces acting on the propeller element on each blade be $A(r)dr$ in the axial flight direction and $F(r)dr$ in the direction opposed to the direction of rotation. Equal reaction forces acting opposite to the flight direction and in the direction of rotation, respectively, are exerted on the medium. These quantities are related to thrust T and torque Q by the relations

$$\left. \begin{aligned} \frac{dT}{dr} &= BA(r) \\ \frac{dQ}{dr} &= BrF(r) \end{aligned} \right\} \quad (8a)$$

or

$$\left. \begin{aligned} T &= B \int_0^R A(r) dr \\ Q &= B \int_0^R rF(r) dr \end{aligned} \right\} \quad (8b)$$

where B is the number of blades and R the length of each blade.

The periodic impulse or reaction experienced at any element of the disk may be expanded in a Fourier series. For simplicity let the element considered first be located on the radial line $\theta = 0$ (the y-axis) and afterwards be located arbitrarily. To start with, assume that the forces are uniformly distributed over the projected width b of the blade element, that is, that the distribution of pressure difference over the blade chord is rectangular. Then in the area element $r dr d\theta$ of the plane of rotation, the forces $A(r)dr \frac{r d\theta}{b}$ and $F(r)dr \frac{r d\theta}{b}$ act on the medium during the time interval in which this element is eclipsed by the projection of the propeller element. If the overlapping of the element starts at $t = 0$, it will end at $t = \tau = \frac{b}{r\Omega}$ and the overlapping of the element will start again by the next blade at $t = \tau_0 = \frac{2\pi}{B\Omega}$, where Ω is the angular velocity of the propeller. The rectangular-type forces experienced at the element of the disk located at $\theta = 0$ by its periodic eclipse by the blade may be developed in a Fourier series:

$$F_1^*(t) = \begin{cases} A(r) \frac{r d\theta}{b} dr & \text{for } 0 < t < \tau \\ 0 & \text{for } \tau < t < \tau_0 \end{cases}$$

$$F_1^*(t) = A_0 + \sum_{m=1}^{\infty} A_m \cos(mB\Omega t - \epsilon_m) \quad (9)$$

and similarly

$$F_2^*(t) = \begin{cases} F(r) \frac{r d\theta}{b} dr & \text{for } 0 < t < \tau \\ 0 & \text{for } \tau < t < \tau_0 \end{cases}$$

$$F_2^*(t) = B_0 + \sum_{m=1}^{\infty} B_m \cos(mB\Omega t - \eta_m) \quad (10)$$

where

$$\left. \begin{aligned} A_m &= \frac{2}{m\pi} A(r) \frac{r}{b} \sin m\pi \frac{\tau}{\tau_0} dr d\theta \\ B_m &= \frac{2}{m\pi} F(r) \frac{r}{b} \sin m\pi \frac{\tau}{\tau_0} dr d\theta \\ \epsilon_m = \eta_m &= m\pi \frac{\tau}{\tau_0} = \frac{mB\Omega\tau}{2\tau_0} \end{aligned} \right\} \quad (11)$$

The constants A_0 and B_0 which correspond to the instantaneous average thrust and torque over the blade element and to the associated momentum shed into the slipstream do not give rise to sound and need not be expressed. The phase angles ϵ_m and η_m , which are small for the lower harmonics, are needed to preserve generality of discussion since $A_m \cos \epsilon_m$ corresponds to the coefficients of pure cosine terms and $A_m \sin \epsilon_m$ to coefficients of pure sine terms in the Fourier series. For the assumed rectangular distribution, ϵ_m and η_m may be observed to be equal to zero if the origin of time is chosen at the overlapping of the center line of the blade by the y-axis since then only a pure cosine series suffices to express the distribution.

The general formulation of interest, where the disk element $r dr d\theta$ is located at an angle θ , may be expressed directly from these results, for, on a second area element $r dr d\theta$ shifted with respect to the first by the angle θ in the rotational direction, there act periodic forces of the same magnitude, but retarded by the time θ/Ω . The corresponding Fourier developments are

$$\left. \begin{aligned} F_1(t) &= F_1^* \left(t - \frac{\theta}{\Omega} \right) = A_0 + \sum_{m=1}^{\infty} A_m \cos(mB\Omega t - mB\theta - \epsilon_m) \\ F_2(t) &= F_2^* \left(t - \frac{\theta}{\Omega} \right) = B_0 + \sum_{m=1}^{\infty} B_m \cos(mB\Omega t - mB\theta - \eta_m) \end{aligned} \right\} \quad (12)$$

The quantity

$$\frac{m\pi\tau}{\tau_0} = \frac{mB\Omega\tau}{2} = \frac{mBb}{2r} \quad (13)$$

is small for the lower harmonics, especially for blade elements not near the hub. Blade elements near the hub, where r is small, are eliminated from consideration since they contribute very little to the air forces.

One may then replace in equation (11) $\sin \frac{m\pi r}{\tau_0}$ by $\frac{m\pi r}{\tau_0}$ so that, noting the relations in equations (8a),

$$\left. \begin{aligned} A_m &\approx \frac{B}{\pi} A(r) dr d\theta \approx \frac{dT}{dr} dr d\theta \\ B_m &\approx \frac{B}{\pi} F(r) dr d\theta \approx \frac{1}{r} \frac{dQ}{dr} dr d\theta \end{aligned} \right\} \quad (14)$$

This approximation, which weights the harmonic content of all the harmonics equally, may be observed to correspond to the case of the thrust and torque distributed over a zero blade width (that is, to the mathematical pulse sometimes termed the Dirac delta function). This approximation becomes relatively less valid when $\frac{m\pi r}{\tau_0}$ exceeds about $\frac{\pi}{4}$

($\sin \frac{\pi}{4} = 0.707$; $\frac{\pi}{4} = 0.785$) or when $4m \frac{r}{\tau_0}$ exceeds about unity; that is, when the order of the harmonic exceeds $\frac{2\Omega}{Bb}$ or, roughly, $1/\text{solidity}$.

Moreover, the assumption of a uniform rectangular distribution of the forces across the blade has been made for convenience, and other distributions may be treated if desired. Some of the possible errors in the assumption leading to equation (14) are discussed briefly by Gutin in reference 1 and are shown to be generally negligible for the lower harmonics. Regier and Hubbard (ref. 4) also discuss this assumption in an illuminating manner. Figure 3, which is taken from reference 4, shows the relative harmonic content of different assumed distributions of the same total load for: (a) the mathematical sharp pulse, (b) a triangular "hat" pulse $\frac{b}{2\pi r} = 0.03$, (c) a rectangular pulse $\frac{b}{2\pi r} = 0.03$, and, (d) a rectangular pulse $\frac{b}{2\pi r} = 0.06$. Blade widths of actual propellers tend to be between cases (c) and (d) for the most effective parts of the propeller disk. The sharp-pulse assumption generally tends to overestimate the magnitude of the higher harmonics. When the proper distribution is known, appropriate correction factors for the required harmonic may, of course, be applied to the magnitude of the results given by the pulse solution.

The formulation in equation (12) need not be limited to the one in which the propeller force distribution is uniform throughout the propeller cycle. If interest should be attached to a nonuniform distribution, as occurs for the propeller yawed or pitched with respect to the flight path or for one experiencing interference effects, it is readily possible to allow for these effects by permitting the amplitude of the distribution to become a function of θ .

The Sound-Pressure Field

The general expressions for the resolution of the forces associated with the thrust and torque on a radial blade element (for example, eqs. (12)) may be put in the usual convenient complex form (whose real part may correspond to the formulation of interest):

$$\left. \begin{aligned} F_1 &= A_0 + \sum_{m=1}^{\infty} A_m e^{i(\omega t - mB\theta - \epsilon_m)} \\ F_2 &= B_0 + \sum_{m=1}^{\infty} B_m e^{i(\omega t - mB\theta - \eta_m)} \end{aligned} \right\} \quad (15)$$

where $\omega = mB\Omega$ and where for the special case of the rectangular pulse distribution the coefficients are given as in equation (11).

With the use of the approximations for A_m and B_m given in equation (14), the periodic forces acting on the medium at the element $r \, dr \, d\theta$ of the disk can be expressed for any given harmonic in the forms

$$\left. \begin{aligned} F_{x,m} &= -\frac{1}{\pi} \frac{dT}{dr} e^{i(\omega t - mB\theta)} dr \, d\theta \\ F_{y,m} &= -\frac{1}{\pi} \frac{1}{r} \frac{dQ}{dr} \sin \theta e^{i(\omega t - mB\theta)} dr \, d\theta \\ F_{z,m} &= \frac{1}{\pi} \frac{1}{r} \frac{dQ}{dr} \cos \theta e^{i(\omega t - mB\theta)} dr \, d\theta \end{aligned} \right\} \quad (16)$$

In the derivation of equation (16), the phase angles ϵ_m and η_m , which can generally be neglected for the lower harmonics, have been put equal to zero, a value which corresponds in the case considered (as has been mentioned) to the choice of $\theta = 0$ to correspond to the overlapping of

the center line of one of the blades at the time $t = 0$. The index m indicates the order of the harmonic considered. As discussed in the preceding section, appropriate factors depending on the harmonic number m , functions of the radius, and, for unsymmetrical loading, functions also of θ may (if known) be applied to the terms in equation (16).

Pressure relations involving integrations over the propeller disk.- The pressure at any point in the free-space field produced by these components of the uniformly moving periodic forces F_x, F_y, F_z is given in equation (6). With the use of the components of force given in equation (16) and by integration over the propeller disk, the total oscillating pressure p for any given harmonic m (the index m will be hereinafter dropped) is obtained from equation (6) as a sum of the pressure due to thrust p_T and that due to torque p_Q as follows:

$$p = p_T + p_Q \quad (17)$$

where

$$p_T = -\frac{1}{4\pi^2} \int_0^R \int_0^{2\pi} \frac{dT}{dr} e^{i(\omega t - mB\theta)} \frac{\partial}{\partial x} \frac{e^{-ik\sigma}}{S} dr d\theta \quad (18)$$

$$p_Q = -\frac{1}{4\pi^2} \int_0^R \int_0^{2\pi} \frac{1}{r} \frac{dQ}{dr} e^{i(\omega t - mB\theta)} \frac{1}{r} \frac{\partial}{\partial \theta} \frac{e^{-ik\sigma}}{S} dr d\theta \quad (19)$$

and where, in the expression for p_Q , the operation $\frac{1}{r} \frac{\partial}{\partial \theta}$ has been used for convenience to replace the equivalent operation $\sin \theta \frac{\partial}{\partial y} - \cos \theta \frac{\partial}{\partial z}$. The indicated differentiations with respect to x and θ can be carried out by use of the expressions for σ and S given in equations (5)

$$\left. \begin{aligned} \frac{\partial}{\partial x} \frac{e^{-ik\sigma}}{S} &= \frac{e^{-ik\sigma}}{S} \left(-\frac{ikM}{\beta^2} - \frac{ikx}{\beta^2 S} - \frac{x}{S^2} \right) \\ \frac{1}{r} \frac{\partial}{\partial \theta} \frac{e^{-ik\sigma}}{S} &= \frac{e^{-ik\sigma}}{S} \left(-\frac{ik}{S} - \frac{\beta^2}{S^2} \right) (y \sin \theta - z \cos \theta) \end{aligned} \right\} \quad (20)$$

Hence,

$$p_T = \frac{e^{i\omega t}}{4\pi^2} \int_0^R \int_0^{2\pi} \frac{dT}{dr} e^{-imB\theta} \frac{e^{-ik\sigma}}{S} \left(\frac{ikM}{\beta^2} + \frac{ikx}{\beta^2 S} + \frac{x}{S^2} \right) dr d\theta \quad (21)$$

and

$$p_Q = \frac{e^{i\omega t}}{4\pi^2} \int_0^R \int_0^{2\pi} \frac{1}{r} \frac{dQ}{dr} e^{-imB\theta} \frac{e^{-ik\sigma}}{S} \left(\frac{ik}{S} + \frac{\beta^2}{S^2} \right) (y \sin \theta - z \cos \theta) dr d\theta \quad (22)$$

Another somewhat simpler expression for p_Q can be obtained from equation (19) by integration by parts with respect to θ

$$p_Q = -\frac{e^{i\omega t}}{4\pi^2} \int_0^R \int_0^{2\pi} \frac{1}{r} \frac{dQ}{dr} e^{-imB\theta} \frac{e^{-ik\sigma}}{S} imB dr d\theta \quad (23)$$

Pressure relations involving effective ring approximation.- Appreciable simplification may be achieved for calculation purposes by making use of the approximations inherent in the assumption of an effective propeller radius R_e so that the integration with respect to r is avoided. Equations (21) and (23) then reduce to

$$p_T = \frac{e^{i\omega t}}{4\pi^2} \int_0^{2\pi} T \left(\frac{ikM}{\beta^2} + \frac{ikx}{\beta^2 S} + \frac{x}{S^2} \right) \frac{e^{-i(mB\theta+k\sigma)}}{S} d\theta \quad (24)$$

and

$$p_Q = -\frac{e^{i\omega t}}{4\pi^2} \int_0^{2\pi} \frac{Q}{R_e^2} imB \frac{e^{-i(mB\theta+k\sigma)}}{S} d\theta \quad (25)$$

where, in both S and σ , the points y_1 and z_1 have the values $y_1 = R_e \cos \theta$, $z_1 = R_e \sin \theta$. In effect, equations (24) and (25) imply that the propeller disk has been replaced by an annular ring in which the entire thrust and torque are concentrated. The effective radius of this ring varies somewhat, as calculation shows, with the load distribution and with the order of the harmonic. Deming (ref. 5) has shown by

calculation in special cases for the static propeller that the ring approximation is a reasonably good one. An effective radius of the order of $0.8R$ is considered reasonable for adoption in initial calculations.

The magnitude of the root-mean-square pressure p_{rms} is of interest, since most sound-recording instruments are calibrated in terms of it. The contribution of the harmonic of order m to the root-mean-square pressure is

$$p_{rms} = \frac{\sqrt{2}}{2} |p_T + p_Q|$$

or

$$p_{rms} = \frac{\sqrt{2}}{8\pi^2} (A^2 + B^2)^{1/2} \quad (26)$$

where

$$A = \int_0^{2\pi} \left\{ \frac{Tx}{S^2} \cos(mB\theta + k\sigma) + \left[T \frac{k}{\beta^2} \left(M + \frac{x}{S} \right) - Q \frac{mB}{Re^2} \right] \sin(mB\theta + k\sigma) \right\} \frac{d\theta}{S}$$

$$B = \int_0^{2\pi} \left\{ -\frac{Tx}{S^2} \sin(mB\theta + k\sigma) + \left[T \frac{k}{\beta^2} \left(M + \frac{x}{S} \right) - Q \frac{mB}{Re^2} \right] \cos(mB\theta + k\sigma) \right\} \frac{d\theta}{S}$$

When rotational symmetry exists as for the condition of symmetrical loading, it is convenient in making the numerical calculations to let the field point be in the xy -plane, an arrangement which can always be attained by suitable choice of the line $\theta = 0$.

Pressure relations for the far field.- A further simplification in the results can be reached if the distance s from the propeller disk $(0, y_1, z_1)$ to the field point $(x, y, 0)$ is large. Then from

$$s^2 = x^2 + (y - y_1)^2 + z_1^2$$

there is obtained

$$s \approx s_0 - \frac{yy_1}{s_0} \quad (27)$$

where $s_0 = \sqrt{x^2 + y^2}$ (the distance from the field point to the center of the propeller disk). It also follows from

$$s^2 = x^2 + \beta^2(y - y_1)^2 + \beta^2 z_1^2$$

that

$$s \approx s_0 - \frac{\beta^2 y y_1}{s_0} \quad (28)$$

where

$$s_0 = \sqrt{x^2 + \beta^2 y^2}$$

If terms of order $1/s^2$ are neglected in comparison with terms of order $1/s$, the sound pressure due to thrust is obtained from equation (24) by use of equations (5) and (28):

$$p_T \approx T \frac{e^{i\omega t}}{4\pi^2} \frac{1}{s_0} e^{-i\frac{k}{\beta^2}(s_0 + Mx)} \frac{1k}{\beta^2} \left(M + \frac{x}{s_0}\right) \int_0^{2\pi} e^{-imB\theta + ik\frac{y}{s_0} R_e \cos\theta} d\theta \quad (29)$$

From the known integral relation

$$\int_0^{2\pi} e^{i\lambda \cos\theta - in\theta} d\theta = 2\pi i^n J_n(\lambda) \quad (30)$$

it follows that

$$p_T = T \frac{e^{i\omega t}}{2\pi s_0} i^{mB} e^{-i\frac{k}{\beta^2}(s_0 + Mx)} \frac{1k}{\beta^2} \left(M + \frac{x}{s_0}\right) J_{mB} \left(\frac{kyR_e}{s_0}\right) \quad (31)$$

Similarly, from equation (25),

$$p_Q = -\frac{Q}{R_e^2} \frac{e^{i\omega t}}{2\pi s_0} i^{mB+1} i^{mBe} e^{-i\frac{k}{\beta^2}(s_0 + Mx)} J_{mB} \left(\frac{kyR_e}{s_0}\right) \quad (32)$$

Observe that the argument of the Bessel function may be replaced by

$$\frac{kyR_e}{S_0} = mBM_{rot} \frac{y}{S_0} \quad (33)$$

where $M_{rot} = \frac{\Omega R_e}{c}$, the Mach number corresponding to the rotational speed at the effective radius. (The far-field approximation and the effective-radius approximation made use of in arriving at eqs. (31) and (32) need not, of course, be made simultaneously, since the required integration of the Bessel functions with respect to the radius may be carried out, at least numerically, without difficulty.)

Introduce the fundamental frequency denoted by $\omega_1 = B\Omega$, so that

$$\omega = mB\Omega = kc = m\omega_1$$

The pressure magnitude for any harmonic m is then given by

$$\begin{aligned} |P| &= |P_T + P_Q| \\ &= \frac{m\omega_1}{2\pi c S_0} \left| T \left(M + \frac{x}{S_0} \right) \frac{1}{\beta^2} - Q \frac{Bc}{\omega_1 R_e^2} \right| J_{mB} \left(\frac{kyR_e}{S_0} \right) \end{aligned} \quad (34)$$

This result may be compared with that for the case of zero forward speed ($M = 0$) given in reference 1:

$$|P| = \frac{m\omega_1}{2\pi c s_0} \left| T \frac{x}{s_0} - Q \frac{Bc}{\omega_1 R_e^2} \right| J_{mB} \left(\frac{kyR_e}{s_0} \right) \quad (35)$$

It can be noted that the forward-speed Mach number affects the torque term containing Q only in the replacing of $s_0 = \sqrt{x^2 + y^2}$ (the distance from the field point to the propeller hub) by the smaller distance $S_0 = \sqrt{x^2 + \beta^2 y^2}$. This substitution occurs both in the argument of the Bessel function and in the outside factor $1/S_0$. The thrust term containing T is more strongly affected, since, in addition to this change, the field effect ahead of and behind the propeller disk is influenced by the term $M + \frac{x}{S_0}$ corresponding to a backward shift by $\frac{x}{S_0} = -M$ and also by an increase because of the factor $1/\beta^2$.

APPLICATION TO A SPECIFIC PROPELLER

In order to give some indication of the effect of forward-speed Mach number on the sound pressure of a propeller, calculations based on equation (26) for the near field and on equation (34) for the far field have been made. For this purpose, a two-blade research propeller having a 10-foot diameter and operating under the various conditions summarized in table I was chosen. As may be noted from this table, the propeller is assumed to operate at constant power; that is, the power coefficient C_p and the torque Q are held constant. As the forward-speed Mach number is changed, the blade angle β_R and consequently the thrust T are changed according to the propeller charts of reference 6 so as to make the assumed conditions consistent with actual test operating conditions. Only the fundamental, the first harmonic $m = 1$, is considered in these examples and the value chosen for the effective radius R_e is $0.8R$ or 4 feet. It should be pointed out that the sound pressure computed from the data of table I would be obtained in pounds per square foot, since these data are given in English units. These values have been converted to dynes per square centimeter in the results given in the figures by multiplication by the approximate conversion factor 480.

Calculations for the near field.- Calculations of the root-mean-square pressure $\left(p_{rms} = \frac{\sqrt{2}}{2} |p| \right)$ based on equation (26) are made for various values of x in the range from $-0.5D$ to $0.5D$ along the line $y = 0.6D$ (6 feet), that is, along a line $1/5$ of the propeller radius from the tip and extending a distance of 1 radius behind to 1 radius ahead of the plane of rotation. These results are shown plotted as a function of x/D for several Mach numbers in figure 4. It can be noted in this figure that, for each Mach number, two peaks generally appear, one ahead of and one behind the plane of rotation. For the set of conditions under consideration (see table I), the highest peak amplitudes of pressure occur just behind the propeller plane at values of x/D in the range from -0.15 to -0.075 . As the Mach number is increased from 0 to 0.4, the peak amplitudes decrease in magnitude, but as the Mach number is increased from 0.4 to 0.9 this trend is reversed and the peak amplitudes increase in magnitude, the peak for $M = 0.9$ being about 1.4 times that for $M = 0$. Also, as M increases from 0 to 0.9, the point at which the highest peak pressure occurs moves somewhat nearer the propeller plane. Thus, the generally severe sound-pressure conditions at take-off ($M \approx 0$) tend to be alleviated in flight at the lower Mach numbers but may be reached again and even exceeded at the higher flight Mach numbers. The calculations for low Mach numbers presented in figure 4, it should be noted, are in substantial agreement with both calculated and measured results of reference 2. The high peak pressures obtained for the highest Mach numbers indicate that, with propeller-driven airplanes, the sound

pressures generated near the tips of the propellers are of significance and of possible concern with regard to both structural considerations and passenger comfort.

Calculations for the far field. - Calculations of the root-mean-square pressures based on equation (34) for various values of x along the line $y = 2D$ (20 feet) are shown plotted in figure 5. The trend with regard to Mach number in this figure is about the same as was noted in figure 4 for $y = 0.6D$, but the relative effect of the forward Mach number appears greater at a distance. However, because of the greater distances in figure 5 than in figure 4, the peak amplitudes are considerably less.

Directional characteristics of the sound field. - For some purposes, especially with regard to calculations for the far field, it is desirable to consider the character of the sound pressure in terms of polar coordinates. For this purpose, substitutions can be made in equation (34) (and eq. (26)) as follows:

$$x = s_o \cos \phi \quad y = s_o \sin \phi \quad s_o = \sqrt{x^2 + y^2} \quad (36)$$

The quantities x/s_o and y/s_o in equation (34) (and eq. (26)) may then be written as

$$\left. \begin{aligned} \frac{x}{s_o} &= \frac{\cos \phi}{\sqrt{1 - M^2 \sin^2 \phi}} \\ \frac{y}{s_o} &= \frac{\sin \phi}{\sqrt{1 - M^2 \sin^2 \phi}} \end{aligned} \right\} \quad (37)$$

With these substitutions, equation (34) becomes

$$|p| = \frac{\rho \omega_1}{2\pi c s_o \sqrt{1 - M^2 \sin^2 \phi}} \left| \frac{T}{\beta^2} \left(M + \frac{\cos \phi}{\sqrt{1 - M^2 \sin^2 \phi}} \right) - Q \frac{Bc}{\omega_1 R_e^2} \right| J_{mB} \left(\frac{k R_e \sin \phi}{\sqrt{1 - M^2 \sin^2 \phi}} \right) \quad (38)$$

Calculations based on equation (38) for the Mach numbers of 0 and 0.8 for a constant value of $s_o = 2D$ are shown plotted as dashed curves

in figure 6. The solid curves in this figure represent results of calculations along the line $y = 2D$ obtained by replacing s_0 by $\frac{y}{\sin \phi}$ with $y = 2D$ in equation (30) for the various Mach numbers considered in figures 4 and 5. A comparison of results of calculations along the line $y = 2D$ with those along the circle $s_0 = 2D$ for $M = 0$ and $M = 0.8$ indicates that, for high Mach numbers (of the order of $M = 0.8$), the peak pressures calculated along a line $y = \text{Constant}$ are about the same as those calculated along the circle with radius equal to the constant value of y . Observe the second pressure peak which has developed in the forward location at $M = 0.9$.

Separate components due to torque and to thrust of the sound field.-

In order to give some indication as to the nature and proportion of sound pressure associated with each of the quantities, thrust T and torque Q , the root-mean-square pressures associated with each of these quantities for $M = 0$ and $M = 0.8$ are plotted for $y = 0.6D$ (6 feet) in figure 7. These plots show, as do equations (26) and (34), that the root-mean-square pressures associated with the propeller torque are symmetrically distributed with respect to the plane of the propeller for all Mach numbers, whereas the root-mean-square pressures associated with the thrust are symmetrical with respect to this plane only for $M = 0$. For the particular propeller and operating conditions under consideration, the amplitudes of pressure associated with thrust for low Mach numbers are higher than those associated with torque, but for high Mach numbers, the opposite is true. In the interpretation of figure 7, it should be recalled that the results depend on the assumed operating conditions and that the torque Q is the same (2,680 ft-lb) in both parts of the figure; whereas the thrust is 1,850 pounds at $M = 0$ and 310 pounds at $M = 0.8$. Plots of this type can be used to obtain the sound pressure for various thrust and torque coefficients for a given propeller, since these coefficients appear as factors in equations (26) and (34) and hence can be normalized.

It is of particular interest to note in the plot for $M = 0.8$ that the peak pressures associated with both thrust and torque are considerably greater than the peak pressure associated with the sum of these quantities. This result indicates that the phase relationship between the two components is, in this case, such that each has a canceling effect on the other. Also in this case, the pressure associated with thrust may have its greatest value ahead of the plane of the propeller; whereas the total pressure has its greatest value behind the plane of the propeller.

The discussion of the figures based on the specific examples illustrates the fact that the results do depend markedly on the assumed operating conditions. Moreover, only the fundamental harmonic ($m = 1$) for the specific two-blade propeller has been illustrated. Trend studies

on effects of higher harmonics, number of blades, and different operating conditions would be of considerable interest. Some preliminary calculations on the sound pressures associated with the fundamental of a six-blade propeller have shown a greater relative effect of the forward-speed Mach number.

CONCLUDING REMARKS

Expressions have been given for the sound-pressure field due to the distribution of thrust and torque for any given harmonic of a rotating propeller in uniform subsonic flight. The general expressions (eqs. (17) to (23)) involve integrations over the propeller disk; approximate expressions for the near field (eqs. (24) to (26)) and for the far field (eqs. (31), (32), and (34)) involve integrations over a ring with an effective radius. The numerical examples have illustrated some free-space sound-pressure results for the fundamental of a specific two-blade propeller under various operating conditions at various forward speeds.

It is pertinent to remark again on some of the limitations of the analysis. The analysis presented utilizes the torque and the thrust distributions, which may be given empirically or theoretically, in such a way as to require that they arise purely from pressures acting normal to the surface of the blades. Empirical values of the thrust and torque include a contribution, generally small, due to skin friction and to separated flow. Some caution is then needed in the use of the results. For example, the empirical torque term is somewhat larger than the torque due purely to normal pressures and, hence, the associated sound result due to torque may be overestimated slightly; similarly, the empirical thrust term may slightly underestimate the sound due to thrust. At high tip speeds there may be significant contributions to the noise due to wave drag associated with the thickness. These contributions are mainly taken into account by the effects of the wave drag on the torque. (Other sound effects of the thickness should be separately calculated and included but these effects have not been explicitly presented herein.)

Another way of looking at the approximation, and perhaps a generally more convenient one for the study of trends, is to consider that the assumed torque and thrust distributions are actual theoretical ones, obtained if necessary by adjustment of the blades of the propeller in a potential flow; and hence the sound-pressure field is that corresponding to the chosen thrust and torque, but in potential flow. Although the sound-pressure field and the aerodynamic velocity field have been considered as separate, it is of interest and of significance that the same concepts leading to the calculation of the sound field (made use of in the form of the acceleration potential) can lead to the linearized aerodynamics of the propeller in compressible flow, including the representation of the vorticity left behind in the wake as a result of spanwise

variation of loading. The theoretical induced drag and the theoretical wave drag (which is a form of acoustic loss) are inherently included in the representation employed.

It may be worthy of repetition that the pressure formulas as given tend to overestimate the contribution of the higher harmonics and that appropriate factors based on chordwise loading can be devised and may be required. Moreover, because of the theoretical (as well as the empirical) change in aerodynamic loading along the blade radially with increasing tip Mach number and forward-speed Mach number, the appropriate factors will change. In addition, the effective radius will be altered with the loading. Thus, although 0.8 blade radius may be suitable as an effective radius for normal loading, a smaller value for the effective radius may be more suitable for conditions where unloading of the tip occurs.

A calculation study of trends under different assumed conditions, the effect of unsymmetrical loading, or of dual propellers, effects of obstacles or boundaries on the free-space results, and experimental confirmations for the in-flight propeller are interesting matters for further investigation.

Langley Aeronautical Laboratory,
National Advisory Committee for Aeronautics,
Langley Field, Va., August 31, 1953.

APPENDIX

THE SOUND-PRESSURE FIELD ASSOCIATED WITH

A UNIFORMLY MOVING FORCE

Derivation of Equations (4) and (6)

Lamb (ref. 3, p. 502) derives from hydrodynamical principles the differential equation satisfied by the pressure condensation s^* in the acoustic field associated with arbitrarily varying fixed forces acting on the medium

$$\begin{aligned}\square^2 s^* &= \left(\frac{\partial^2}{\partial x^2} + \frac{\partial^2}{\partial y^2} + \frac{\partial^2}{\partial z^2} - \frac{1}{c^2} \frac{\partial^2}{\partial t^2} \right) s^* \\ &= \frac{1}{c^2} \left(\frac{\partial X}{\partial x} + \frac{\partial Y}{\partial y} + \frac{\partial Z}{\partial z} \right)\end{aligned}\quad (A1)$$

where Lamb's X, Y, Z are actually the extraneous forces per unit volume divided by the density ρ . (In effect, Lamb is dealing here with the acceleration potential.) In terms of the perturbation pressure $p = \rho c^2 s^*$ the equation is

$$\begin{aligned}\square^2 p &= \text{div } \bar{F} \\ &= \frac{\partial F_x}{\partial x} + \frac{\partial F_y}{\partial y} + \frac{\partial F_z}{\partial z}\end{aligned}\quad (A2)$$

where \bar{F} is the arbitrary force per unit volume having components F_x, F_y, F_z . Lamb shows that if the periodic force $Ae^{i\omega t}$ is imagined concentrated on an infinitely small space at (x_1, y_1, z_1) and to be in the direction of x , the pressure at the field point (x, y, z) (the distance s from the location of the force) is given by

$$p = \frac{A}{4\pi} \frac{\partial}{\partial x} \frac{e^{i\omega(t - \frac{s}{c})}}{s}\quad (A3)$$

where

$$s = \sqrt{(x - x_1)^2 + (y - y_1)^2 + (z - z_1)^2}$$

so that the concentrated force is equivalent to a double source or acceleration doublet whose axis is in the direction of the force. For a general harmonically periodic force \bar{F} having components F_x, F_y, F_z varying in time as $e^{i\omega t}$

$$\begin{aligned} p &= \frac{1}{4\pi} (\bar{F} \cdot \nabla) \frac{e^{iks}}{s} \\ &= \frac{1}{4\pi} \left(F_x \frac{\partial}{\partial x} + F_y \frac{\partial}{\partial y} + F_z \frac{\partial}{\partial z} \right) \frac{e^{-iks}}{s} \end{aligned} \quad (A4)$$

where $k = \frac{\omega}{c}$.

For an arbitrary time-dependent concentrated force $\bar{F}(t)$ located at (ξ, η, ζ) , the pressure at field point (x, y, z) can be expressed as

$$\begin{aligned} p &= \frac{1}{4\pi} \operatorname{div} \frac{\bar{F}(\xi, \eta, \zeta, t - \frac{s}{c})}{s} \\ &= \frac{1}{4\pi} \left[\frac{\partial}{\partial x} \frac{F_x(t - \frac{s}{c})}{s} + \frac{\partial}{\partial y} \frac{F_y(t - \frac{s}{c})}{s} + \frac{\partial}{\partial z} \frac{F_z(t - \frac{s}{c})}{s} \right] \end{aligned} \quad (A5)$$

where the differentiations affect the result only through the variable s .

The extension to a moving concentrated force may, within the framework of small-perturbation theory, be made in several ways - for example, as mentioned in reference 7. One formal procedure utilized by Küssner, for example, makes use of the invariance properties of the wave equation and utilizes combined Galilean and Lorentz transformations. The following direct procedure given briefly in reference 7 is believed to be of intrinsic interest, as it represents a simplification in Prandtl's procedure (ref. 8) for the case of moving constant source distributions, a procedure which consists of scheduling a succession of fixed sources in a path to act consecutively one after the other so as to represent in effect the desired source moving along its path. Let the arbitrary concentrated force act only as an impulse during an infinitesimal interval at time $t = \tau$. The impulse may be written as

$$\bar{F}(t)\delta(t - \tau) \quad (A6)$$

where the impulse function $\delta(\tau) = 0$ for $\tau \neq 0$ and is characterized for $\tau = 0$ as having unit area with respect to τ . The useful property of the impulse function of "sifting or selecting" a value of a function is exhibited by the following relation (see, for example, ref. 9, p. 61):

$$\int_{-\infty}^{\infty} f(\sigma - \tau)\delta(\tau)d\tau = \int_{-\infty}^{\infty} f(\tau)\delta(\sigma - \tau)d\tau = f(\sigma) \quad (A7)$$

Let a succession of such impulses act, one following the other, in a path, points along which are given in space-fixed coordinates by

$$\xi = \xi(\tau) \quad \eta = \eta(\tau) \quad \zeta = \zeta(\tau)$$

The effect at time t of all such impulses which act before the time t is then given from Lamb's result (eq. (A5)) as

$$p = \frac{1}{4\pi} \operatorname{div} \int_{-\infty}^t \frac{\bar{F}(\tau)}{s} \delta\left(t - \tau - \frac{s}{c}\right) d\tau \quad (A8)$$

where, as has been defined, there is a nonzero contribution to the integral only for values of τ defined by the characteristic relation

$$t - \tau = \frac{s}{c} = \frac{1}{c} \sqrt{[x - \xi(\tau)]^2 + [y - \eta(\tau)]^2 + [z - \zeta(\tau)]^2} \quad (A9)$$

which expresses the distance between the source point and the field point in terms of the time of travel of the outgoing waves.

The integral in equation (A8) corresponds to a summation of temporary fixed sources. To represent the case of uniform rectilinear motion with velocity V in the positive x -direction, let the sources be located on the ξ -axis and flow consecutively one after the other at the positions

$$\xi = V\tau \quad \eta = 0 \quad \zeta = 0 \quad (A10)$$

so that for $\tau = -\infty$ the source is located at $\xi = -\infty$ and for $\tau = 0$ the source is located at the origin. It follows that the distance between source point and field point is

$$s = \sqrt{(x - V\tau)^2 + y^2 + z^2} \quad (A11)$$

Replace in equation (A8) the variable τ by θ where

$$t - \tau - \frac{s}{c} = \theta \quad (\text{A12})$$

By the sifting property of the δ -function (eq. (A7)) the integral will have a value only for $\theta = 0$ and equation (A8) becomes

$$p = \frac{1}{4\pi} \operatorname{div} \left[\frac{\bar{F}(\tau)}{s} \frac{d\tau}{d\theta} \right]_{\theta=0} \quad (\text{A13})$$

where the quantity within the bracket is now to be evaluated. Equations (A11) and (A12) give a quadratic equation for τ which, on choice of the solution that leads to $\tau < t$ and with $\theta = 0$, gives

$$\tau = \frac{1}{\beta^2} \left(t - \frac{Vx}{c^2} - \frac{S}{c} \right) \quad (\text{A14})$$

where

$$s = \sqrt{(x - Vt)^2 + \beta^2(y^2 + z^2)}$$

$$\beta = \sqrt{1 - M^2}$$

$$M = \frac{V}{c}$$

Equations (A11) and (A12) also give

$$\frac{1}{s} \frac{d\tau}{d\theta} = \frac{c}{cs - V(x - V\tau)}$$

where replacing s by its characteristic value $c(t - \tau)$ from equation (A9) and replacing τ by its value given in equation (A14) yields, for $\theta = 0$,

$$\frac{1}{s} \frac{d\tau}{d\theta} = \frac{1}{S} \quad (\text{A15})$$

where S is defined in equation (A14). Equation (A13) becomes

$$p = \frac{1}{4\pi} \operatorname{div} \frac{\bar{F} \left[\left(t - \frac{V}{c^2} x - \frac{S}{c} \right) \frac{1}{\beta^2} \right]}{S} \quad (\text{A16})$$

This result is referred to space-fixed coordinates; it is finally desired also to express this result in terms of a field point (x_0, y_0, z_0) of a coordinate system moving uniformly along with the source located at x_1, y_1, z_1 so that one may put

$$x - Vt = x_0 - x_1 \quad y = y_0 - y_1 \quad z = z_0 - z_1$$

After this substitution is made, the zero subscripts may be dropped to yield as the end result corresponding to equation (A5) for the source and the coordinate system in uniform rectilinear motion:

$$p = \frac{1}{4\pi} \operatorname{div} \frac{\bar{F}\left(t - \frac{\sigma}{c}\right)}{S} \quad (\text{A17})$$

where

$$S = \sqrt{(x - x_1)^2 + \beta^2 \left[(y - y_1)^2 + (z - z_1)^2 \right]}$$

$$\sigma = \frac{M(x - x_1) + S}{\beta^2}$$

$$\beta = \sqrt{1 - M^2}$$

Equation (A17) corresponds to the result given in equation (4) of the analysis. For the periodic harmonic force \bar{F} varying as $e^{i\omega t}$, it may be expressed in the form

$$p = \frac{1}{4\pi} (\bar{F} \cdot \nabla) \frac{e^{-ik\sigma}}{S} \quad (\text{A18})$$

which is equivalent to equation (6) of the analysis. Equations (A17) and (A18) are the sought-for generalizations of equations (A5) and (A4) of the appendix, for the case where the disturbance and the field point are in uniform rectilinear motion. Comparison of these equations shows at once that s is replaced by S in the amplitude and by σ in the phase. A geometric interpretation of these quantities is shown in figure 1 and discussed in the analysis following equation (5).

Remarks On the Case of the Moving Disturbance
and the Fixed Observer

A few remarks are in order on the significance of equation (A16). In this equation, the field point (x,y,z) is given in space-fixed coordinates while the disturbance force (or propeller) is in the in-flight condition moving with velocity V in the positive x -direction. Its location is given by $x_1 = Vt$, $y_1 = 0$, $z_1 = 0$ so that at $t = 0$ it is located at the origin. It may be observed that the distance between disturbance and field point S is numerically the same whether given by the relation in equation (A16) or (A17). Hence, the pressure magnitude at any observer location for a sound-radiating element of the in-flight propeller is the same as that for the observer moving along with the propeller, provided the proper instantaneous distance between observer and propeller is used. However, there will be a difference in the frequency perceived by the observer. This frequency will be that for the case of the uniformly moving observer modified by the Doppler effect; thus, the frequency of each harmonic is modified by $c/(c + V_r)$, where V_r is the component of the propeller forward speed (with proper sign: minus, for approaching, plus for receding from, the observer) in the acoustical direction from the observer to, say, for the far approximation, the hub of the propeller. The acoustical direction is not quite that from the observer to the propeller location; it actually points from the observer to the location of the propeller when the sound which reaches the observer was emitted (direction \overline{QP} rather than \overline{QO} in fig. 1). The Doppler frequency factor $c/(c + V_r)$ is given geometrically in figure 1 by the ratio of $\frac{QR}{QP} = \frac{s}{\sigma}$.

REFERENCES

1. Gutin, L.: On the Sound Field of a Rotating Propeller. NACA TM 1195, 1948. (From Phys. Zeitschr. der Sowjetunion, Bd. 9, Heft 1, 1936, pp. 57-71.)
2. Hubbard, Harvey H., and Regier, Arthur A.: Free-Space Oscillating Pressures Near the Tips of Rotating Propellers. NACA Rep. 996, 1950. (Supersedes NACA TN 1870.)
3. Lamb, Horace: Hydrodynamics. Sixth ed., Cambridge Univ. Press, 1932, p. 502.
4. Regier, Arthur A., and Hubbard, Harvey H.: Status of Research on Propeller Noise and Its Reduction. Jour. Acous. Soc. Am., vol. 25, no. 3, May 1953, pp. 395-404.
5. Deming, Arthur F.: Propeller Rotation Noise Due to Torque and Thrust. NACA TN 747, 1940.
6. Gray, W. H.: Wind-Tunnel Tests of Single- and Dual-Rotating Tractor Propellers at Low Blade Angles and of Two- and Three-Blade Tractor Propellers at Blade Angles Up to 65°. NACA WR L-316, 1943. (Formerly NACA ARR, Feb. 1943.)
7. Garrick, I. E.: On Moving Sources in Nonsteady Aerodynamics and in Kirchhoff's Formula. Proc. First U. S. Nat. Cong. Appl. Mech. (Chicago, Ill., 1951.), A.S.M.E., 1952, pp. 733-739.
8. Prandtl, L.: Theorie des Flugzeugtragflügels im zusammendrückbaren Medium. Luftfahrtforschung, Bd. 13, Nr. 10, Oct. 12, 1936, pp. 313-319.
9. Van der Pol, Balth., and Bremmer, H.: Operational Calculus Based on the Two-Sided Laplace Integral. Cambridge Univ. Press, 1950.

BIBLIOGRAPHY

1. Lynam, E. J. H., and Webb, H. A.: The Emission of Sound by Airscrews. R. & M. No. 624, British A.C.A., 1919.
2. Bryan, G. H.: The Acoustics of Moving Sources With Application to Airscrews. R. & M. No. 684, British A.R.C., 1920.
3. Hart, Morris D.: The Aeroplane as a Source of Sound. R. & M. No. 1310, British A.R.C., 1930.
4. Gutin, L.: On the Sound Field of a Rotating Propeller. NACA TM 1195, 1948. (From Phys. Zeitschr. der Sowjetunion, Bd. 9, Heft 1, 1936, pp. 57-71.)
5. Ernsthausen, W.: The Source of Propeller Noise. NACA TM 825, 1937. (From Luftfahrtforschung, Bd. 13, Nr. 12, Dec. 20, 1936, pp. 433-440.)
6. Deming, A. F.: Noise From Propellers With Symmetrical Sections at Zero Blade Angle, II. NACA TN 679, 1938.
7. Deming, Arthur F.: Propeller Rotation Noise Due to Torque and Thrust. NACA TN 747, 1940.
8. Ernsthausen, Wilhelm: Der Einfluss aerodynamischer Eigenschaften auf Schallfeld und Strahlungsleistung einer Luftschraube. Luftfahrtforschung, Bd. 18, Lfg. 8, Aug. 20, 1941, pp. 289-304.
9. Yudin, E. Y.: On the Vortex Sound From Rotating Rods. NACA TM 1136, 1947. (From Zhurnal Tekhnicheskoi Fizike, vol. 14, no. 9, 1944, p. 561.)
10. Shirokov, M. F.: The Sound of a Moving Aeroplane Propeller. Comptes Rendus Acad. Sci. URSS, vol. XLIX, no. 8, 1945, pp. 565-567.
11. Blokhintsev, D. I.: Akustika neodnorodnoy dvizhushcheyasya sredy. (Acoustics of a Nonhomogeneous Moving Medium.) OGIZ, Gosudarstvennoe Izdatel'stvo, Tekhniko-Teoreticheskoy Literatury (Moscow, Leningrad), 1946. (Translation available from Research Analysis Group, Brown University (Contract N7-onr-35808), Aug. 1952.)
12. Küssner, H. G.: Lösungen der klassischen Wellengleichung für bewegte Quellen. UM Nr. 3217, Deutsche Luftfahrtforschung (Göttingen), 1945.
13. Kuessner, Hans Georg, and Billings, Heinz: Unsteady Flow. VI of Hydro- and Aerodynamics, Albert Betz, ed., ATI No. 72854, CADO, Wright-Patterson Air Force Base, May 1950, pp. 141-198.

14. Ernsthausen, Wilhelm: Der rotierende Tragflügel als Strahlungsproblem. Z.a.M.M., Bd. 31, Nr. 1/2, Jan./Feb. 1951, pp. 20-35.
15. Hubbard, Harvey H., and Regier, Arthur A.: Free-Space Oscillating Pressures Near the Tips of Rotating Propellers. NACA Rep. 996, 1950. (Supersedes NACA TN 1870.)
16. Hubbard, Harvey H., and Lassiter, Leslie W.: Sound From a Two-Blade Propeller at Supersonic Tip Speeds. NACA Rep. 1079, 1952. (Supersedes NACA RM 151C27.)
17. Von Gierke, H. E.: Physical Characteristics of Aircraft Noise Sources. Jour. Acous. Soc. Am., vol. 25, no. 3, May 1953, pp. 367-378.
18. Regier, Arthur A., and Hubbard, Harvey H.: Status of Research on Propeller Noise and Its Reduction. Jour. Acous. Soc. Am., vol. 25, no. 3, May 1953, pp. 395-404.

TABLE I
 SEA-LEVEL OPERATING CONDITIONS FOR A 10-FOOT-DIAMETER
 TWO-BLADE PROPELLER (DATA FROM REFERENCE 6)

$$[P = 815 \text{ hp}; C_p = 0.10; Q = 2,680 \text{ lb-ft}; k = 0.29686]$$

M	V/nD	β_R , deg	C_T	η , percent	T, ft-lb
0	0	24	0.11	0	1,850
.1	.42	26	.11	46	1,850
.2	.84	28	.094	75	1,600
.3	1.26	33	.065	85	1,090
.4	1.68	37	.052	87	875
.5	2.10	42	.041	86	690
.6	2.52	47	.032	80	580
.7	2.94	50	.025	70	420
.8	3.36	53	.0185	62	310
.9	3.78	56	.0122	46	205

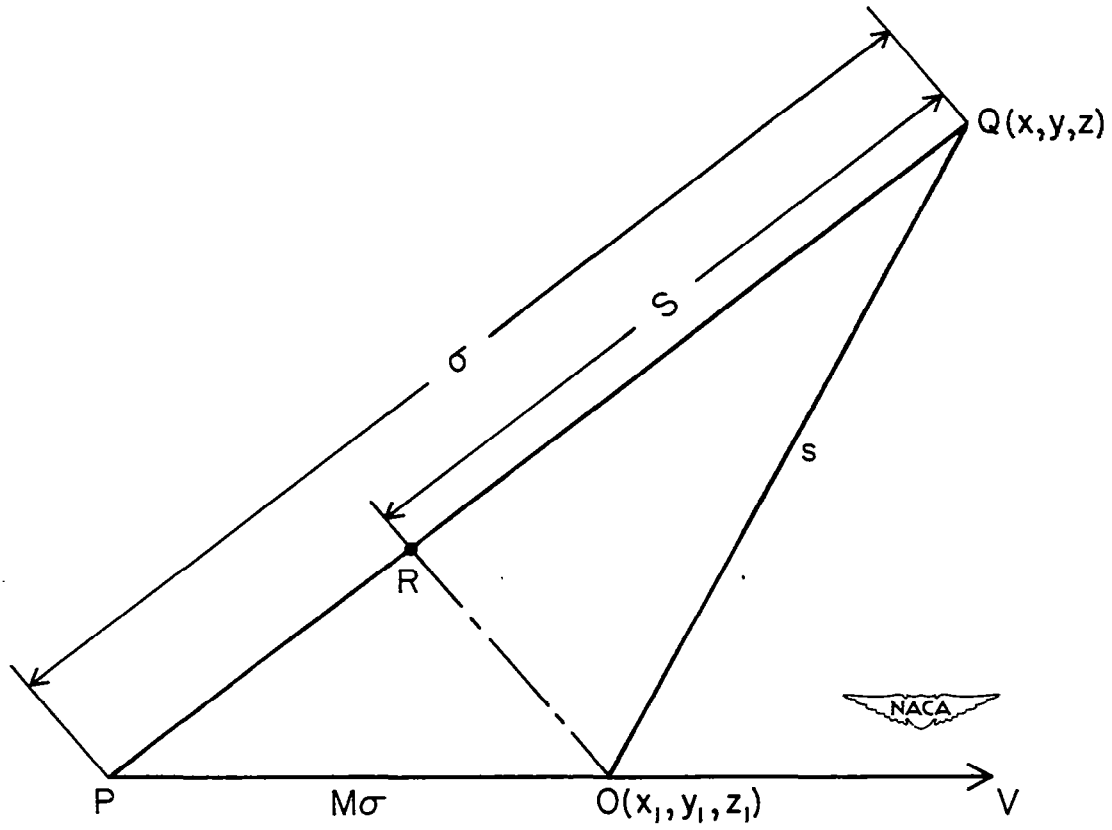


Figure 1.- Geometric representation of s , S , and σ .

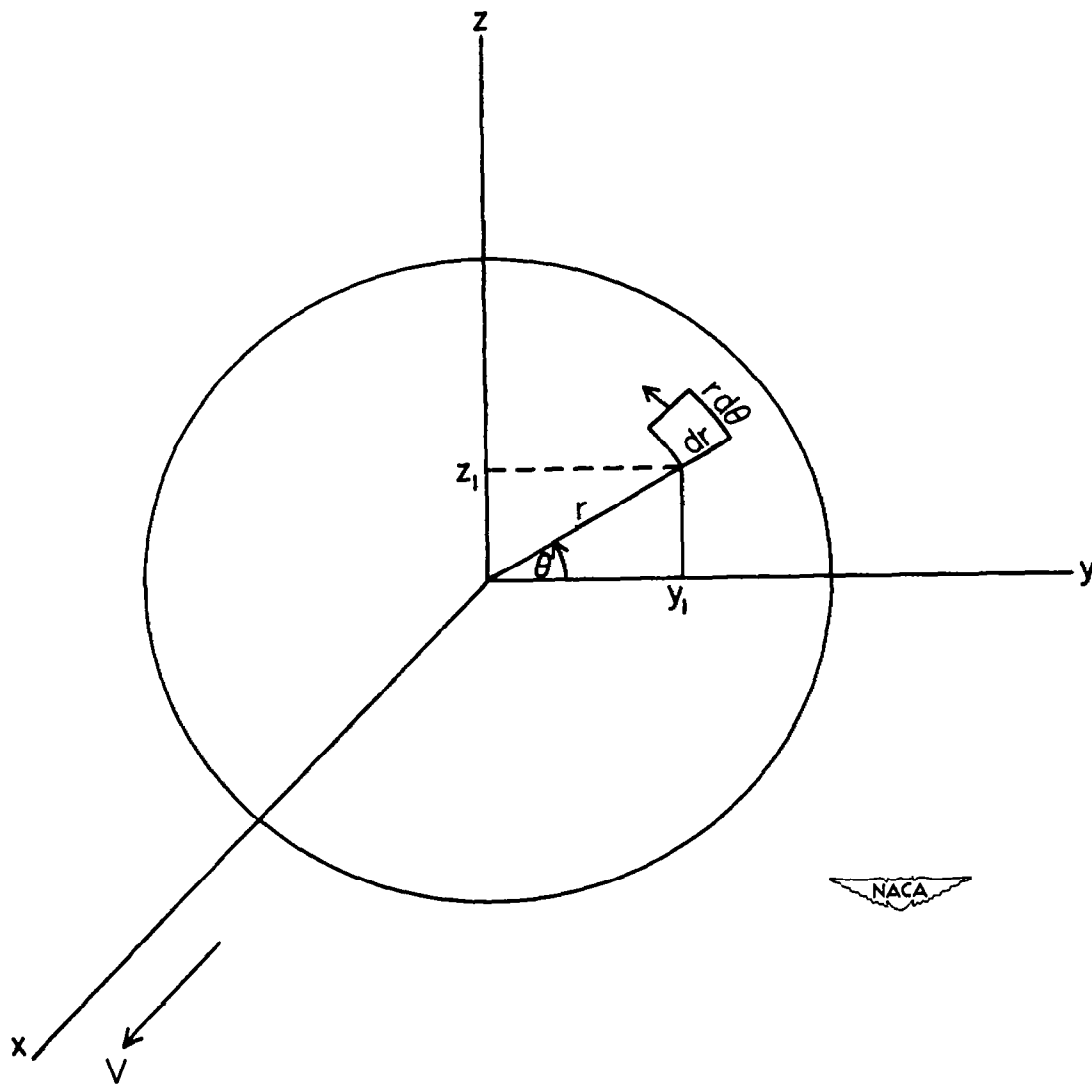
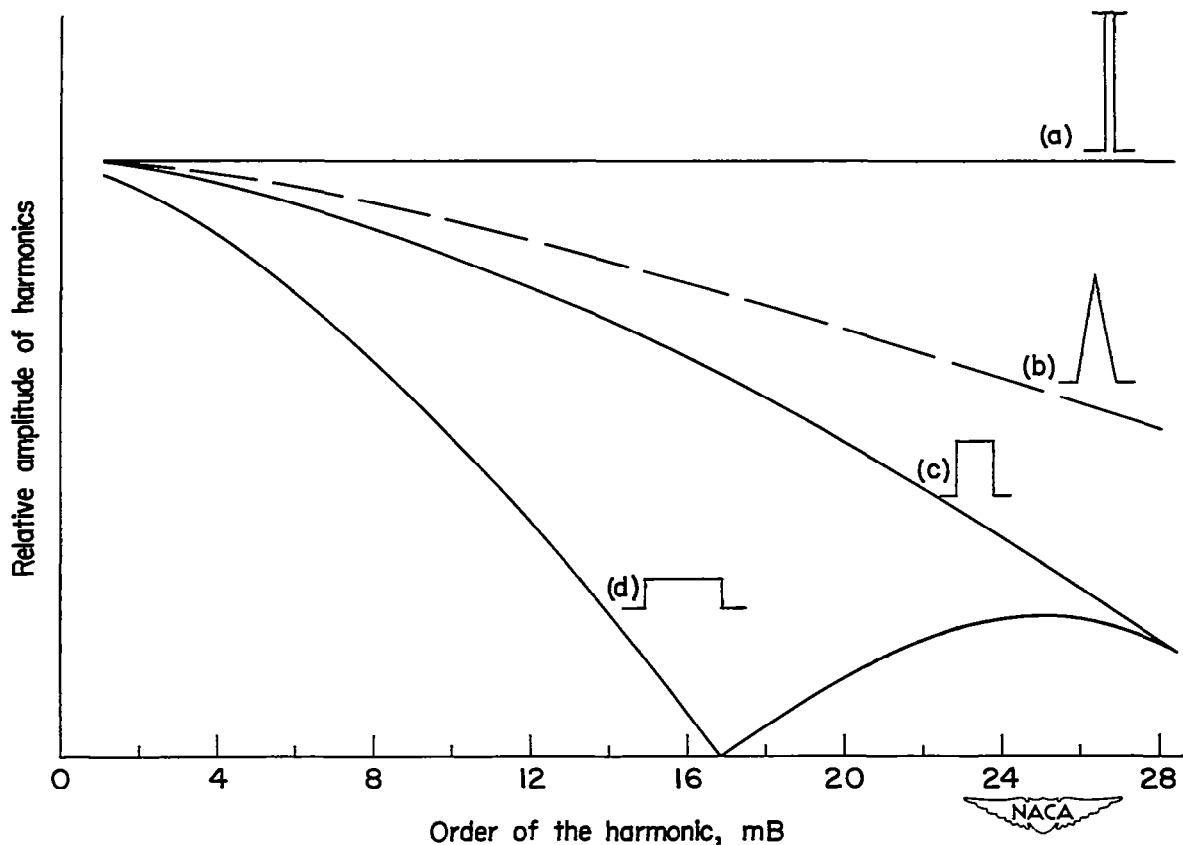


Figure 2.- Propeller disk and coordinate system.



(a) Sharp pulse.

(b) Triangular pulse. $\frac{b}{2\pi r} = 0.03.$

(c) Rectangular pulse. $\frac{b}{2\pi r} = 0.03.$

(d) Rectangular pulse. $\frac{b}{2\pi r} = 0.06.$

Figure 3.- Effect of impulse shape on the relative amplitudes of the harmonics.

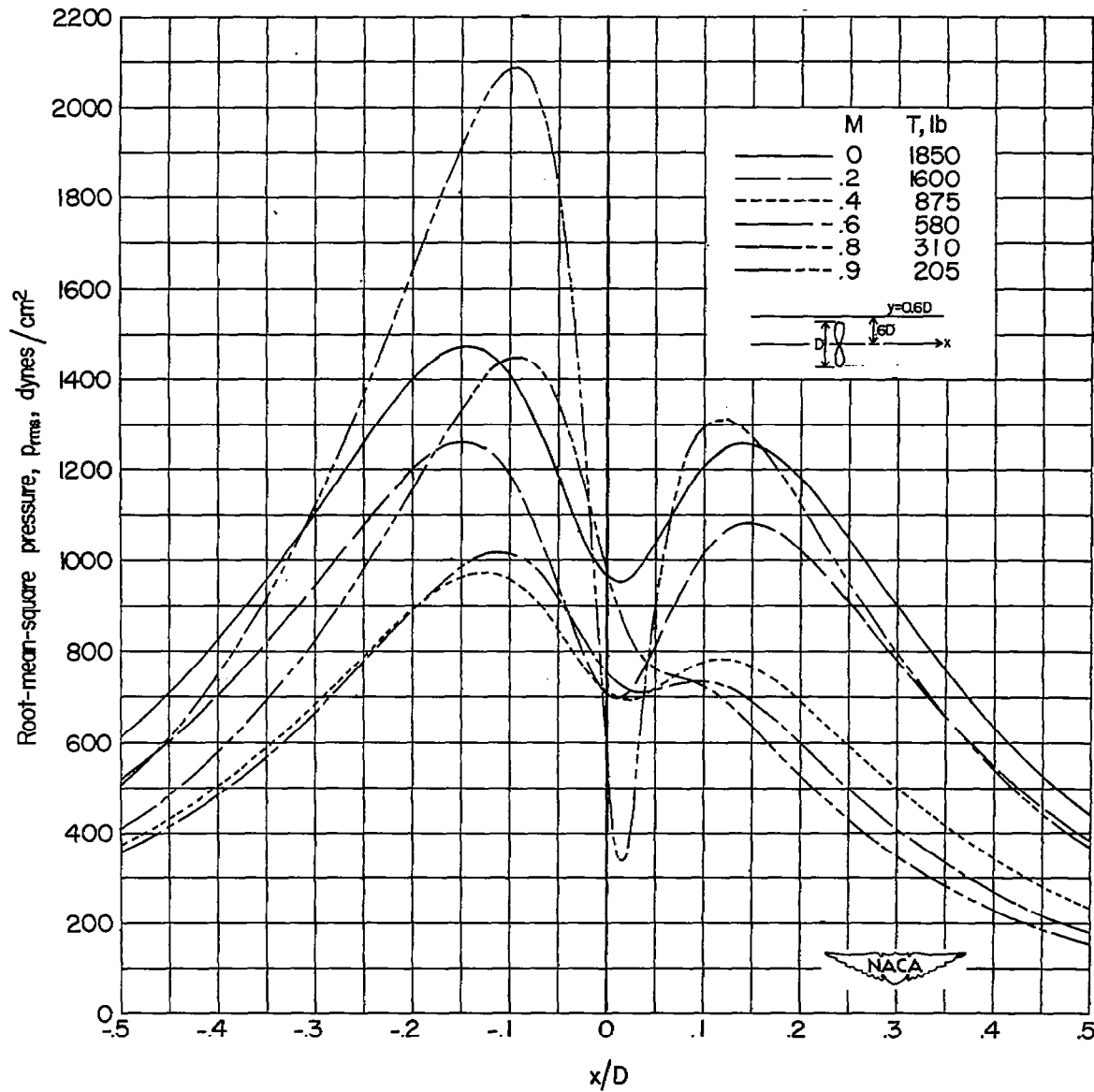


Figure 4.- Distribution of the root-mean-square pressures for the fundamental ($m = 1$) of a two-blade 10-foot-diameter propeller at several forward-speed Mach numbers. $C_p = 0.10$; $k = 0.29686$; $y = 6$ feet. (Operating conditions of propeller given in table I.)

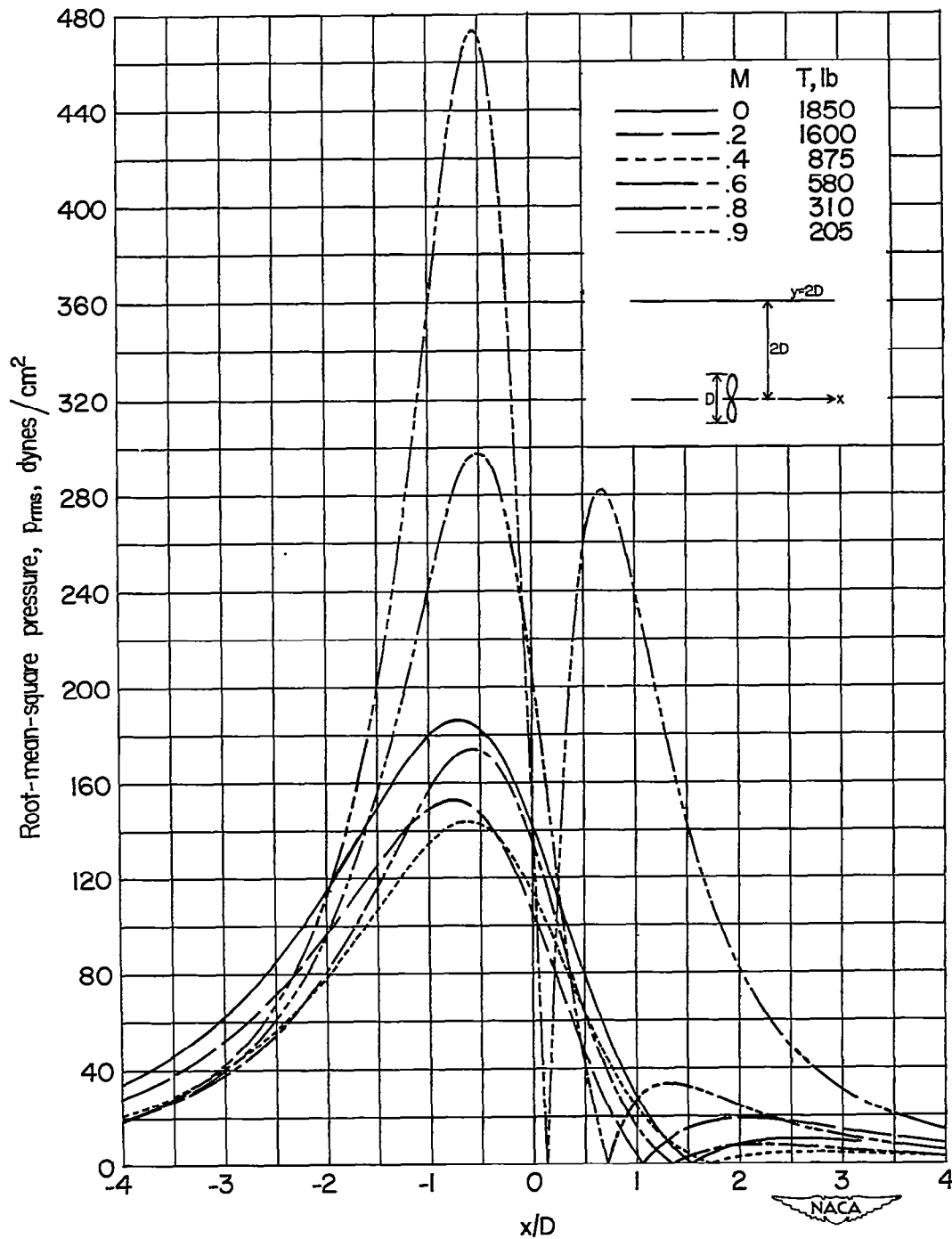


Figure 5.- Distribution of the root-mean-square pressures for the fundamental ($m = 1$) of a two-blade 10-foot-diameter propeller at several forward-speed Mach numbers. $C_p = 0.10$; $k = 0.29686$; $y = 20$ feet. (Operating conditions of propeller given in table I.)

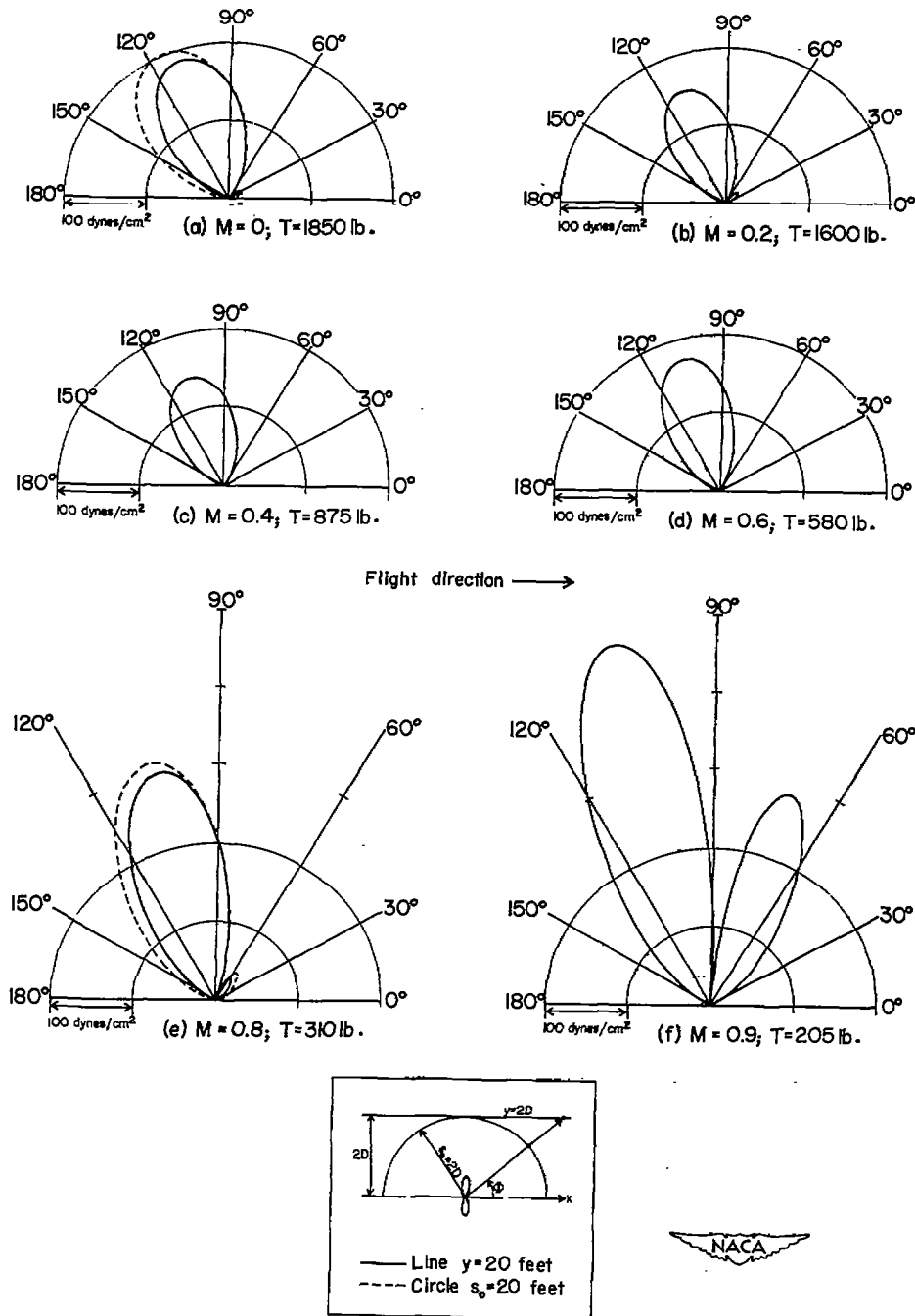


Figure 6.- Polar diagrams of the root-mean-square pressures calculated along a line $y = 20$ feet and along a circle $s_0 = 20$ feet for a two-blade, 10-foot-diameter propeller at several forward-speed Mach numbers. $C_p = 0.10$; $m = 1$; $k = 0.29686$. (Operating conditions of propeller given in table I.)

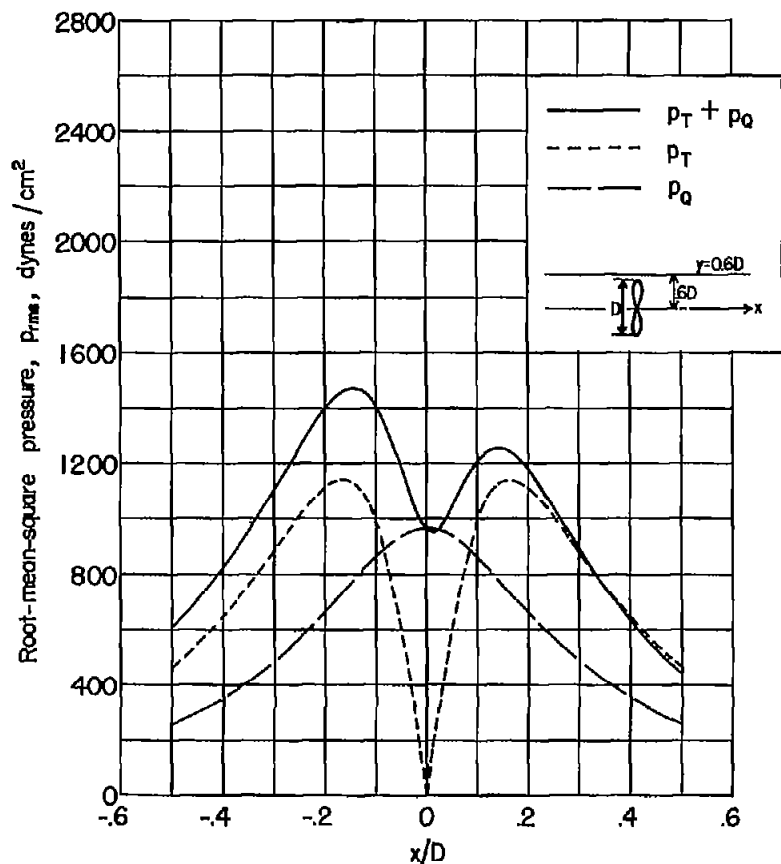
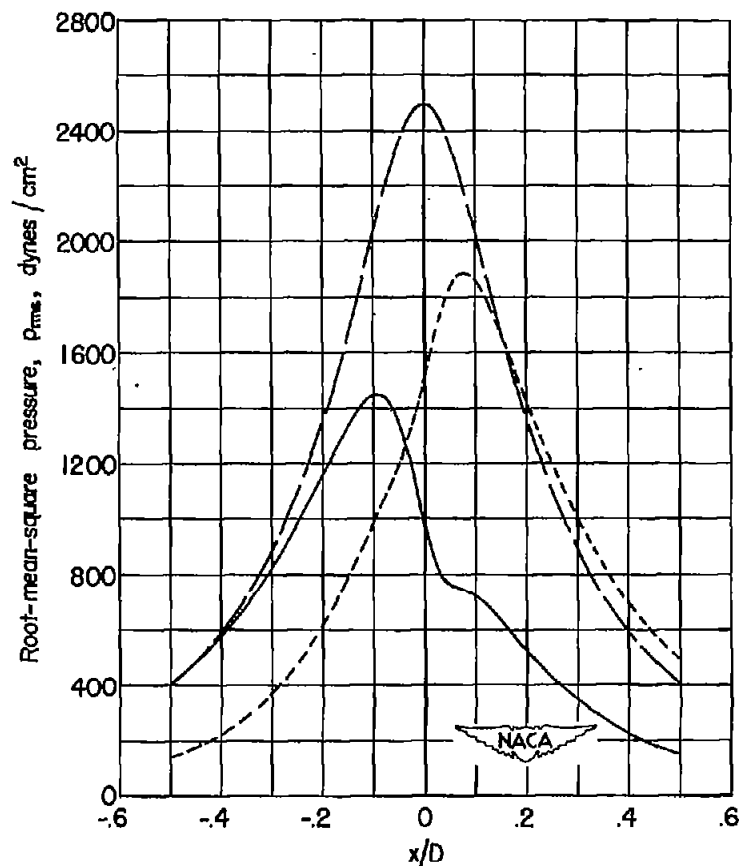
(a) $M = 0$; $T = 1850$ lb.(b) $M = 0.8$; $T = 310$ lb.

Figure 7.- Distribution of the root-mean-square total pressures and the root-mean-square pressures associated with thrust and torque for a two-blade, 10-foot-diameter propeller at forward-speed Mach numbers of 0 and 0.8. $C_p = 0.10$; $m = 1$; $k = 0.29686$; $y = 6$ feet. (Operating conditions of propeller given in table I.)